

中国激光

基于 OCT 的昆虫心脏功能参数自动检测定量分析方法

王秀丽^{1,2}, 杜若瑄¹, 姚晓天^{1,2}, 苏亚^{1,2,3*}, 崔省伟^{1,2,3}, 郝鹏^{1,2}, 杨丽君¹, 段兵兵^{1,2}

¹河北大学物理科学与技术学院, 河北 保定 071002;

²河北省光学感知技术创新中心, 河北 保定 071002;

³河北大学生命科学与绿色发展研究院, 河北 保定 071002

摘要 心血管疾病是一种严重威胁人类健康的常见病。目前常用手段之一是以昆虫为模式生物, 利用 RNAi 等技术抑制特定基因表达, 通过表型检测或监测其心脏功能参数等来开展此类疾病致病机理的研究。光学相干层析技术(Optical Coherence Tomography, OCT)因其无创、实时、高分辨率等特点, 被成功应用于昆虫等模式生物的心脏功能检测方面。但目前的检测计算方法仍存在效率低、对图像质量要求高、参数测量不准确等问题, 尤其不适用于生物实验中大样本量的检测分析。提出一种基于 OCT 的昆虫心脏功能参数高速自动检测定量分析计算方法。该算法结合 OCT 心脏 M-Mode 图, 采用人机交互的模式确定种子点所在的位置, 通过自动分割图像、划分目标区域等一系列处理, 可以快速准确地测量心脏舒张末期直径(EDD)、收缩末期直径(ESD)、舒张末期面积(EDA)、收缩末期面积(ESA)及心率(HR)等心脏功能参数。该方法有助于提升高通量生物样本检测中致病基因的筛查和分析效率, 对以昆虫为模式生物的心血管疾病研究具有重要的价值。

关键词 生物技术; 光学相干层析; 昆虫; 模式生物; 心脏功能参数

中图分类号 TN247

文献标志码 A

DOI: 10.3788/CJL202249.2007202

1 引言

心血管疾病是危害人类健康的重大疾病之一。目前, 中国心血管病患病率仍处于持续上升阶段, 据推算心血管病患病人数已达 3.3 亿人^[1]。因此, 关于心血管疾病的致病基因及其遗传变异功能的研究也愈发重要。果蝇、飞蝗等昆虫作为经典的模式生物, 在心脏发育过程中具有与人类相似的基因调控机制^[2-3], 且具有发育周期短、可控性强等特性, 已成为研究心脏功能及心脏疾病致病基因的有力工具^[4-5]。研究人员提出了多种评估昆虫心脏功能的方法, 如多传感心电图^[6]、原子力显微镜^[7]、电起搏应力法^[8]等, 但这些方法均属于有创检测, 即需要对蝗虫进行解剖, 露出背血管进行测量, 准确性易受有创操作的影响, 而且实验后昆虫个体即死亡, 不能对同一活体进行持续检测。

因此, 具有无创、可持续监测优势的检测手段对评估昆虫等模式生物的心脏发育情况及研究致病基因和表型尤为重要。光声断层成像技术(PAT)可无创检测活体心脏等器官及表征心肌梗死^[9-10]。此外, 光学相干层析技术(OCT)因具有无创、实时、高分辨率等

特点, 被广泛应用于生物医学检测方面, 但相比于 PAT 的 200 μm 左右的空间分辨率, OCT 的分辨率为十几微米, 因此 OCT 更适于检测昆虫等小型模式生物的发育情况及表型变化等。OCT 主要利用低相干干涉原理, 通过检测不同深度的后向散射信号, 可对生物组织和其他非均匀散射体的内部结构进行高分辨率的成像^[11-12]。OCT 具有超高分辨率, 可对胚胎进行二维和三维断面实时成像, 能够获取生物体胚胎在不同发育阶段的心脏生物医学形态特征及生理信息^[13-19], 还可用于血管及组织的三维可视化成像^[20-21]。此外, OCT 也应用于果蝇等模式生物的心脏疾病致病基因及其活动特征的定量评估研究^[22-23]。但关于心脏功能参数(如心率等)的测量, 仍需要通过 M-Mode 图进行人工计算, 不仅耗费时间, 而且容易出错。Fink 等^[24]开发了一种运动分析算法, 该方法将心脏跳动的高速光学记录与半自动分析相结合, 可以定量测量心脏功能参数, 但对显微镜和相机的要求较高, 只适用于具有高分辨率的成像装置, 不具有普适性。Guo 等^[25]利用一种半自动分割算法分析果蝇心脏搏动收缩舒张参数, 但由于层析图像边缘模糊或噪声的影响, 在提取图

收稿日期: 2021-12-07; 修回日期: 2022-01-07; 录用日期: 2022-02-11

基金项目: 国家自然科学基金(62105091)、河北省重点研发计划(19Z2109D, 20542201D)、河北省自然科学基金(F2020201041, F2021201016)、河北省高等学校科学技术研究基金项目(QN2019035)、河北大学“新医科”教学改革项目(2020XYKY08)

通信作者: *suya@hbu.edu.cn

像边缘时易出现不平滑的情况,因此参数测定不准确。半自动分割算法、罗盘算子等可实现感兴趣区域的快速分割,但在分割过程中会出现目标区域内噪声或灰度不均匀引起的欠分割或过分割的情况。为了解决该问题,研究人员开发了基于主成分分析的监督学习方法来训练腔室轮廓,活动轮廓分割算法、自动水平集分割算法、深度学习、自适应分水岭算法以及基于形态学特征的IVOCT内腔自动分割方法使腔室和边缘分割更加准确^[26-33]。Rahman等^[34]利用U-Net分割模型提取曲线信息的准确位置,使用多项式回归进行后处理以获得曲线边界信息。Valerio^[35]通过寻找边缘检测阈值和形态学操作的最佳组合来提取感兴趣区域。因此,研究更高效率的自动检测算法以适应高通量的模式生物致病基因筛查及其表型分析成为目前亟须解决的问题之一。

蝗虫作为研究心脏疾病的模式生物,具有易操作、可塑性强、发育周期短等特点,可以利用OCT的无创、分辨率高的优势,实现蝗虫胚胎期心脏发育的动态监测。我们之前利用OCT实时、无损伤和三维成像的特性,对蝗虫活体胚胎发育和遗传改良的生物表型现象进行检测,特别是利用RNAi基因干扰技术进行胚胎期间操作以及孵化后的表型观察^[13]。本文在团队之前关于昆虫胚胎发育及其基因表达调控的表型测定的工作^[13, 36]基础上,以飞蝗为模式生物,提出了一种新的自动快速定量计算昆虫心脏功能参数的方法,能够对心脏舒张末期直径(EDD)、收缩末期直径(ESD)、舒张末期面积(EDA)、收缩末期面积(ESA)及

心率(HR)等心脏功能参数进行准确的定量测量,该方法尤其适用于大样本量(通常数量 ≥ 30)的生物体检测。本文所提出的方法是利用在OCT成像特点基础上得到的M-Mode图来进行数据分析。M-Mode图像常用于超声心动图中,用于评估心脏动力学,如收缩同步性、心肌工作及心室内血流动力学等^[24]。随着OCT研究的愈加深入,其图像采集深度最大可达到米级^[37]。因此,本文提出的基于OCT的心脏功能参数自动检测定量分析方法在未来也将有着更广泛的应用空间。

2 方法与原理

2.1 实验仪器及数据采集

实验所用仪器为高速扫频OCT,中心波长为1300 nm,在组织中的轴向和横向分辨率分别为12 μm 和25 μm ,平均输出功率为10 mW,扫描速率为16 kHz。

对蝗虫胚胎心脏腔室的某一固定位置[图1(a)白色竖虚线标志处]沿y方向连续进行160次A-scan,相当于沿yz面进行B-scan,结果如图1(b)所示。在此位置重复进行720次B-scan(扫描时间为10 s),则获得了心脏腔室在不同时间的舒张和收缩图像。图1(b)、(c)分别为蝗虫胚胎心脏舒张末期和收缩末期的二维B-scan截面图。图像扫描深度为3 mm,在深度方向即z方向进行扫描,扫描结果包含512个像素点。扫描范围为0 mm \times 2 mm \times 3 mm,得到的像素体数据为720 pixel \times 160 pixel \times 512 pixel,如表1所示。

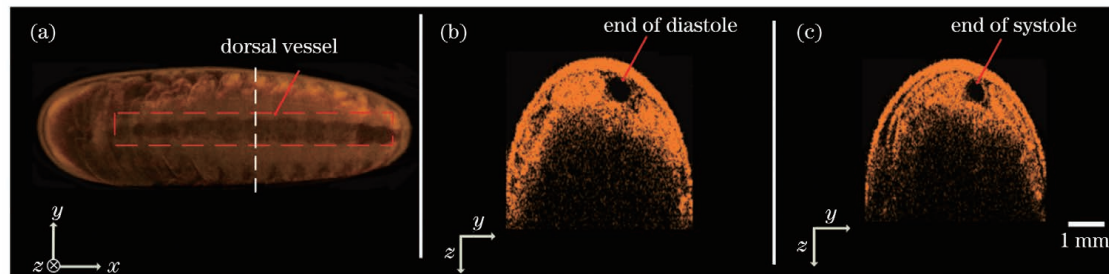


图1 飞蝗胚胎的OCT扫描图像。(a) 胚胎三维投影图;胚胎心脏(b)舒张末期和(c)收缩末期的二维B-scan截面图

Fig. 1 Typical OCT images of locust embryo. (a) 3D projection image of locust embryo; 2D B-scan cross-sections of embryonic heart at (b) end of diastole and (c) end of systole

表1 OCT扫描参数设置

Table 1 Scanning parameter setting of OCT

Scanning direction	Field of view /mm	Size /pixel
x (transverse)	0	720
y (longitudinal)	2	160
z (axial)	3	512

2.2 定量计算方法

昆虫心脏功能参数的定量检测计算方法如图2所示。将采集得到的3D数据,以时间序列展开,得到胚

胎心脏腔室的M-Mode图。如图3(a)所示,M-Mode图的横坐标为扫描时间。M-Mode图最早被应用于人体的超声波心脏检测,通过计算心脏功能参数,对相关心血管疾病进行诊断。通过对M-Mode图进行灰度变换,再进行阈值选取、区域生长、边界识别和特征峰提取等一系列操作,即可计算得出心率、舒张末期直径及收缩末期直径等参数。

2.2.1 灰度变换

由于随机噪声的影响,原始的OCT图像质量较差,需要进行图像的预处理。对图像进行灰度变换,可以减小低频噪声的影响,提高图像的信噪比。假设原

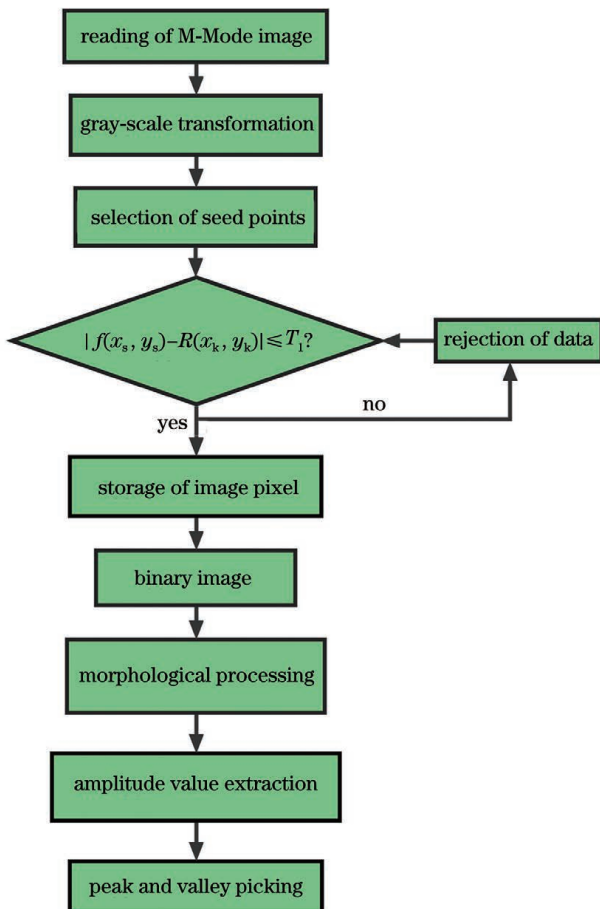


图2 心脏功能参数的定量检测算法流程图

Fig. 2 Flow chart of quantitative detection algorithm for cardiac function parameters

图像 $f(x, y)$ 的灰度变换范围为 $[a_1, a_2]$, 变换后的图像 $T(x, y)$ 的灰度范围为 $[b_1, b_2]$, 本文选取的灰度变换映射范围为 $[0.2, 0.9]$ 。

2.2.2 基于阈值分割的区域生长

在灰度变换后的 M-Mode 图中创建一组初始种子点, 用于提取心脏腔室内边缘。设置胚胎心脏腔室为待分割区域 $f(x, y)$, 采用人机交换模式选定区域内某一点为种子点 $R(x_k, y_k)$, 选定的心脏腔区域的灰度均值(m)和标准差(σ)分别为

$$m = \frac{1}{n} \sum_{i=1}^n I_i(x, y), \quad (1)$$

$$\sigma = \sqrt{\frac{1}{n} \sum_{i=1}^n |I_i(x, y) - m|^2}, \quad (2)$$

式中: n 是待分割区域像素点个数; $I_i(x, y)$ 是待分割区域内第 i 个像素点位置 (x, y) 处的像素值。

因此选定图像的灰度变化阈值(T_1)的一致性判别条件为

$$T_1 = \left(1 - \frac{\sigma}{m}\right) \cdot T_c, \quad (3)$$

式中: T_c 是由生长环境决定的, 取值范围是 $0.3 \sim 0.5$ 。

对于待分割区域 $f(x, y)$, 生长准则为

$$|f(x_s, y_s) - R(x_k, y_k)| \leqslant T_1, \quad (4)$$

式中: $f(x_s, y_s)$ 为待测生长点邻域内的灰度值; $R(x_k, y_k)$ 为种子点的像素值。

对种子点的八邻域进行索引赋值, 满足生长准则的位置及其像素值自动保存到图像 $J(x, y)$ 中, 由此可得到一个二值化的图像:

$$J(x, y) = \begin{cases} 1, & I \leqslant T_1, \\ 0, & \text{others} \end{cases}, \quad (5)$$

式中: I 为待分割区域中像素点的灰度值。

通过式(3)确定下一种子点所在位置, 进行统计迭代, 更新状态, 对对应索引位置的像素值进行赋值, 在经过图像灰度值翻转后, 可得到对应的二值化的图像 $J'(x, y)$ 。

2.2.3 形态学处理

由于蝗虫胚胎心脏腔轮廓不平滑性和随机噪声的影响, 腔内及边缘的像素灰度值可能会出现局部最大值, 导致腔内和腔边缘出现亮点。腔内亮点的存在会导致腔内形成不连通区域, 进而无法提取心脏腔的振幅值; 而对于腔边缘, 这些亮点的堆叠会导致腔边缘变得粗糙不平滑, 从而所提取的腔振幅值的准确性受到影响。

空洞是一组背景像素, 无法通过图像边缘背景填充来连通目标区域。本文先对二值化图像不连通区域进行填充, 再采用结构元素对二值化图进行腐蚀运算, 之后再进行膨胀运算。形态学处理可在一定程度上平滑腔边缘, 填补腔内的空洞, 使腔内连通。

对于已进行形态学处理的二值化图像, 通过统计 A-scan 中逻辑值为 0 的像素点的个数, 并利用已知的单个像素点的大小, 即可获得不同时刻心脏的搏动幅度, 进而计算得出心率、舒张末期直径及收缩末期直径等参数。本文采集图像的单个像素点在 z 方向上的尺寸约为 $6 \mu\text{m}$, 受像素点计数方式的影响, 测量的不准确性为 1 个像素点, 即精度为 $6 \mu\text{m}$ 。

2.3 实验设计

蝗虫成虫将卵产于湿润的沙土中, 当卵中胚胎发育到第 7 天时, 实验人员将蝗卵从沙土中取出, 用乙醇对卵表面进行消毒后放置于琼脂糖培养皿中, 将培养皿置于 30°C 的恒温培养箱中继续培育孵化。在第 9 天, 通过 OCT 能够清晰地观测到蝗卵内胚胎幼体的一整条背血管, 如图 1(a)矩形框所示。背血管是蝗虫胚胎的心脏, 是维持胚胎生命活动的重要器官。因此, 通过 OCT 监测胚胎背血管中膨大心室的收缩图像变化即可定量测得心脏功能参数。图 1(a)为发育到第 9 天的蝗虫胚胎沿 z 方向的投影图, 图 1(b)和图 1(c)分别表示蝗虫胚胎舒张末期和收缩末期的二维 B-scan 图像, 其中空腔部分为胚胎的心室。本文对一组发育时间为 $9 \sim 14$ d 的 30 只蝗虫胚胎进行了 OCT 活体成像监测, 并利用心脏功能参数自动检测方法进行了定量分析计算。

3 结果与讨论

通过对原始的 M-Mode 图[图 3(a)], 双向箭头所指位置表示心脏最大舒张直径和最小收缩直径]进行灰度变换处理, 可以得到去除低频噪声的 M-Mode 图[图 3(b)], 然后选取胚胎心脏腔内的任意一点[图 3(c)中的红色圆点]作为初始的种子点, 图 3(d)是在规定的区域生长准则下得到的二值化的区域生长结

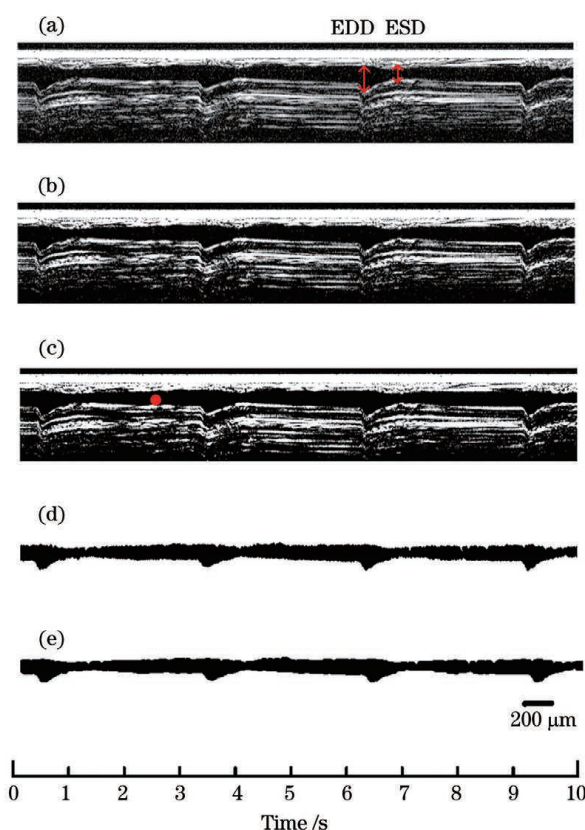


图 3 飞蝗胚胎发育到第 9 天时的 OCT M-Mode 图像。(a)未经处理的原始图;(b)经过灰度变换后的 M-Mode 图;(c)加入种子点的灰度变换 M-Mode 图;(d)阈值分割处理后的 M-Mode 图;(e)经过形态学处理后的 M-Mode 图;(f)蝗虫胚胎心脏的振幅图;(g)利用峰值提取从图 3(f)中找到的极值点

Fig. 3 OCT M-Mode images of 9-day locust embryo. (a) Original image before treatment; (b) M-Mode image after grayscale transformation; (c) M-Mode image after grayscale transformation added with seed point; (d) M-Mode image after threshold segmentation; (e) M-Mode image after morphologic processing; (f) amplitude image of locust embryonic heart; (g) extreme points obtained by peak value extraction from Fig. 3(f)

我们利用 OCT 获得了蝗虫胚胎心脏在 10 s 内的 M-Mode 图, 并结合阈值分割区域生长算法完整提取了心脏舒张和收缩振幅值, 相关参数的自动提取可取代大量的重复性工作, 并生成客观、准确和全面的指标参数。通过该算法可以定量计算得到蝗卵的心率、最大舒张末径、最小收缩末径、心动周期(HP)、舒张间期(DI)和收缩间期(SI)等心脏功能评价指标参数。

图 4 所示为蝗虫在胚胎期的心脏发育情况。随着发育天数的增加, 胚胎心率明显加快。胚胎在发育到第 9 天时, 背血管(心脏)基本发育成型, 并能够被 OCT 观测到, 心率为 $(28 \pm 5) \text{ beat} \cdot \text{min}^{-1}$, 在发育到第 14 天即将孵化出壳时, 心率值达到 $(116 \pm 9) \text{ beat} \cdot \text{min}^{-1}$ 。

果。可以看到, 灰度分布不均匀导致边缘处出现毛刺, 从而所提取的心脏搏动振幅的准确性受到影响。为解决这一问题, 我们引入了形态学处理, 对腔体边缘进行平滑处理, 如图 3(e)所示。此时, 将每一列 A-scan 逻辑值为 0 的像素点总数乘以其长度, 即可得到对应的振幅图[图 3(f)]。如图 3(g)所示, 利用峰值提取算法找到极值点后, 可计算 HR、EDD 和 ESD 等心脏参数指标。

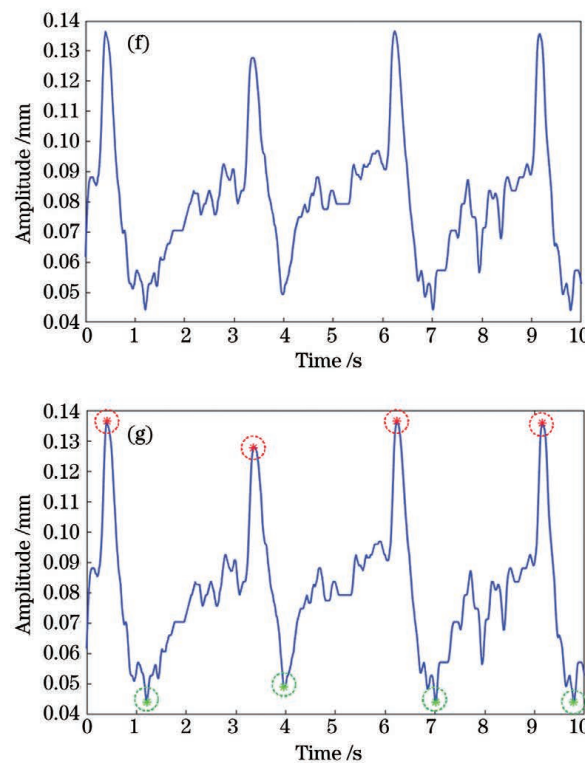


图 4 蝗虫胚胎心率

Fig. 4 Heart rate of locust embryo

相比果蝇 $300 \text{ beat} \cdot \text{min}^{-1}$ 左右的心率^[20], 蝗虫的心率与人类心率更为接近, 因此其作为模式生物也更适合于人体心脏疾病的研究。

图5所示为30只蝗虫胚胎心脏的平均最大EDD和最小ESD随发育天数的变化情况。可以看出,蝗虫胚胎的平均最大EDD和最小ESD在其心脏初步成型期(9~10天)和即将破壳期(13~14天)增长速度较快,而在正常发育期(10~13天)增长速度相对较为平缓。

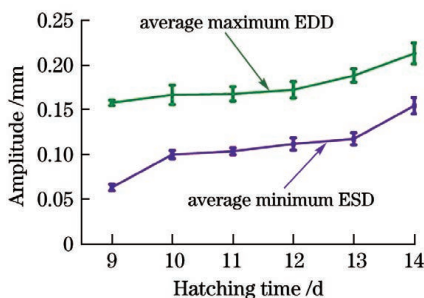


图5 蝗虫胚胎心脏的平均最大EDD和最小ESD随发育天数的变化

Fig. 5 Average maximum EDD and minimum ESD versus hatching time of locust embryonic heart

将原始图像由M-Mode图换为胚胎心脏截面的B-scan图像,按照2.2节的步骤,则可计算得到蝗虫胚

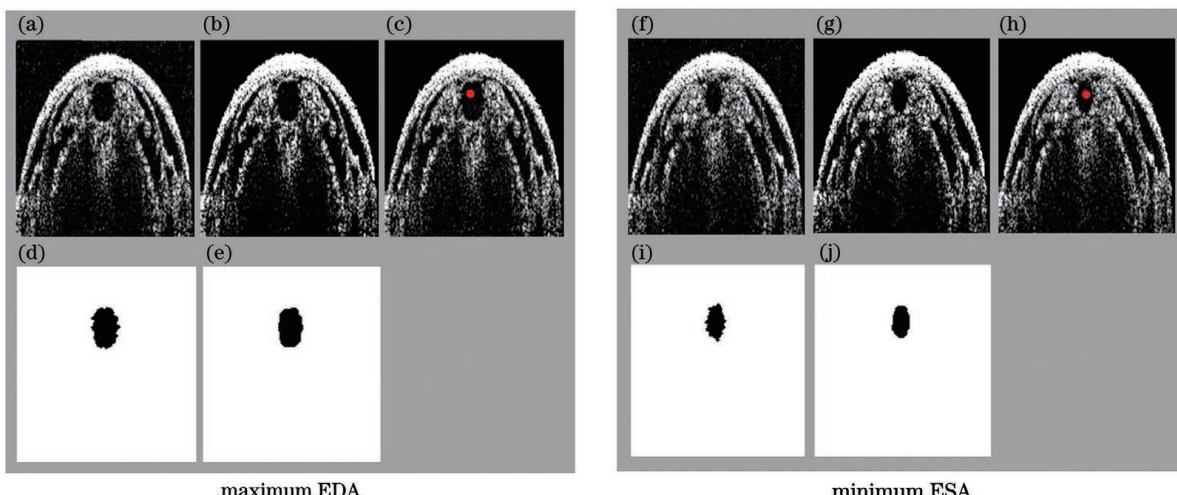


图6 蝗虫胚胎心脏最大EDA与最小ESA计算示意图。(a)(f)原始图像;(b)(g)灰度变换后的图像;(c)(h)加入种子点后的图像;(d)(i)阈值分割处理后的结果图;(e)(j)经形态学处理后的图像

Fig. 6 Calculation diagrams of maximum EDA and minimum ESA of locust embryonic heart. (a)(f) Original images; (b)(g) images after grayscale transformation; (c)(h) images added with seed point; (d)(i) result images after threshold segmentation; (e)(j) images after morphologic processing

图7所示为胚胎在不同发育时间下的心脏平均最大EDA和最小ESA,其变化趋势与EDD和ESD的变化趋势具有一致性,均随着发育天数的增加呈现增长趋势。

4 结 论

选取蝗虫作为评估心脏功能的模式生物,提出了基于OCT的新的自动快速定量计算昆虫心脏功能参数的方法。该方法可有效解决传统检测算法中效率低、对图像质量要求高、参数测量不准确等问题。所提方法在以昆虫为模式生物的心血管疾病研究方面具有重要的参考价值。

胎心脏最大舒张末期面积和最小收缩末期面积,如图6所示。由于原始图像中存在散粒噪声[图6(a)和图6(e)],噪声会对局部区域图像造成干扰,使待分割区域与周围像素之间的灰度差异减小,从而导致在后期处理时,若阈值选取不当,有可能会出现过分割或欠分割的现象,进而丢失大量信息或造成信息冗余。如果目标边界模糊,生长终止延后,可能造成过分割。如果目标区域内的灰度分布不均匀,生长提前终止,可能造成欠分割。利用灰度变换使待分割区域与背景的灰度差增大,去除造影图内的噪声,使目标区域与外围区域之间的边界更加清晰,从而改善图像分割效果。因此,在阈值分割前对图像进行灰度变换可以减小随机噪声造成的处理不准确[图6(b)和图6(g)]。从图6(d)和图6(i)可以看出,在阈值分割处理后的图像中,分割区域的周围(心脏腔)仍存在很多的毛刺,这是空腔边缘的不平滑性造成的。故还需通过形态学处理对分割图像周围进行平滑处理,最后得到理想的胚胎心脏腔室区域的图像。将统计的该区域像素点个数乘以单个像素点的面积,即可计算得出心脏腔室区域的面积。

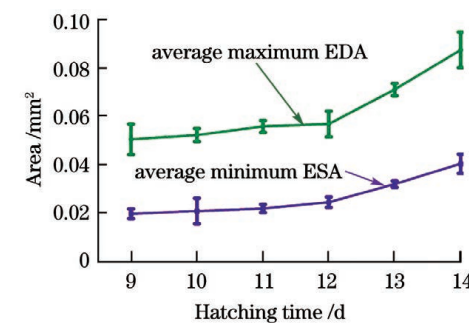


图7 蝗虫胚胎心脏平均最大EDA和最小ESA随发育天数的变化

Fig. 7 Average maximum EDA and minimum ESA versus hatching time of locust embryonic heart

参 考 文 献

- [1] 王增武, 胡盛寿.《中国心血管健康与疾病报告2019》要点解读[J].中国心血管杂志, 2020, 25(5): 401-410.
Wang Z W, Hu S S. Interpretation of report on cardiovascular health and diseases in China 2019 [J]. Chinese Journal of Cardiovascular Medicine, 2020, 25(5): 401-410.
- [2] Badisco L, Huybrechts J, Simonet G, et al. Transcriptome analysis of the desert locust central nervous system: production and annotation of a *Schistocerca gregaria* EST database [J]. PLoS One, 2011, 6(3): e17274.
- [3] Bodmer R. Heart development in *Drosophila* and its relationship to vertebrates[J]. Trends in Cardiovascular Medicine, 1995, 5(1): 21-28.
- [4] Qu H, Cui L, Rickers-Haunerland J, et al. Fatty acid-dependent expression of the muscle FABP gene-comparative analysis of gene control in functionally related, but evolutionary distant animal systems[J]. Molecular and Cellular Biochemistry, 2007, 299(1/2): 45-53.
- [5] Huang K, Miao T, Chang K, et al. Impaired peroxisomal import in *Drosophila* oenocytes causes cardiac dysfunction by inducing *upd3* as a peroxikine [J]. Nature Communications, 2020, 11: 2943.
- [6] Sláma K. A new look at the comparative physiology of insect and human hearts[J]. Journal of Insect Physiology, 2012, 58(8): 1072-1081.
- [7] Ocorr K, Reeves N L, Wessells R J, et al. KCNQ potassium channel mutations cause cardiac arrhythmias in *Drosophila* that mimic the effects of aging [J]. Proceedings of the National Academy of Sciences of the United States of America, 2007, 104(10): 3943-3948.
- [8] Wessells R J, Bodmer R. Screening assays for heart function mutants in *Drosophila*[J]. Biotechniques, 2004, 37(1): 58-60, 62, 64.
- [9] Lü J, Peng Y, Li S, et al. Hemispherical photoacoustic imaging of myocardial infarction: *in vivo* detection and monitoring [J]. European Radiology, 2018, 28(5): 2176-2183.
- [10] 李娇, 李帅, 陈冀景, 等. 非接触光声成像研究进展及其在生物医学上的应用[J]. 中国激光, 2021, 48(19): 1918005.
Li J, Li S, Chen J J, et al. Progress and biomedical application of non-contact photoacoustic imaging [J]. Chinese Journal of Lasers, 2021, 48(19): 1918005.
- [11] Bille J F. High resolution imaging in microscopy and ophthalmology[M]. Cham: Springer, 2019.
- [12] Jang I K. Cardiovascular OCT imaging[M]. Cham: Springer, 2020.
- [13] Su Y, Wei L Y, Tan H, et al. Optical coherence tomography as a noninvasive 3D real time imaging tool for the rapid evaluation of phenotypic variations in insect embryonic development [J]. Journal of Biophotonics, 2020, 13(2): e201960047.
- [14] 毛广娟, 林燕萍, 陈婷如, 等. 幼年到成年斑马鱼大脑的OCT活体三维可视化[J]. 中国激光, 2020, 47(12): 1207002.
Mao G J, Lin Y P, Chen T R, et al. OCT *in vivo* three-dimensional visualization of zebrafish brains from juvenile to adult[J]. Chinese Journal of Lasers, 2020, 47(12): 1207002.
- [15] Raghunathan R, Singh M, Dickinson M E, et al. Optical coherence tomography for embryonic imaging: a review [J]. Journal of Biomedical Optics, 2016, 21(5): 050902.
- [16] Wang S, Larina I V, Larin K V. Label-free optical imaging in developmental biology[J]. Biomedical Optics Express, 2020, 11(4): 2017-2040.
- [17] Ma Z H, Du L L, Wang Q Y, et al. Changes in strain and blood flow in the outflow tract of chicken embryo hearts observed with spectral domain optical coherence tomography after outflow tract banding [J]. Proceedings of SPIE, 2013, 8593: 859305.
- [18] Lopez A L, Wang S, Larina I V. Embryonic mouse cardiodynamic OCT imaging [J]. Journal of Cardiovascular Development and Disease, 2020, 7(4): 42.
Boppert S A, Tearney G J, Bouma B E, et al. Noninvasive assessment of the developing *Xenopus* cardiovascular system using optical coherence tomography [J]. Proceedings of the National Academy of Sciences of the United States of America, 1997, 94(9): 4256-4261.
- [19] Wei B, Yuan Z L, Tang Z L. Three-dimensional imaging of tumor tissues based on photothermal optical coherence tomography[J]. Acta Optica Sinica, 2020, 40(4): 0411002.
- [20] 刘颖, 杨亚良, 岳献. 光学相干层析血管造影术及其在眼科学中的应用[J]. 激光与光电子学进展, 2020, 57(18): 180002.
Liu Y, Yang Y L, Yue X. Optical coherence tomography angiography and its applications in ophthalmology [J]. Laser & Optoelectronics Progress, 2020, 57(18): 180002.
- [21] Liu Y, Yang Y L, Yue X. Optical coherence tomography angiography and its applications in ophthalmology [J]. Laser & Optoelectronics Progress, 2020, 57(18): 180002.
- [22] Zurauskas M, Bradu A, Ferguson D R, et al. Closed loop tracked Doppler optical coherence tomography based heart monitor for the *Drosophila melanogaster* larvae[J]. Journal of Biophotonics, 2016, 9(3): 246-252.
- [23] Alex A, Li A R, Zeng X X, et al. A circadian clock gene, cry, affects heart morphogenesis and function in *drosophila* as revealed by optical coherence microscopy[J]. PLoS One, 2015, 10(9): e0137236.
- [24] Fink M, Callol-Massot C, Chu A, et al. A new method for detection and quantification of heartbeat parameters in *Drosophila*, zebrafish, and embryonic mouse hearts [J]. BioTechniques, 2009, 46(2): 101-113.
- [25] Guo S Y, Liao F T, Su M T, et al. Semiautomatic and rapid quantification of heartbeat parameters in *Drosophila* using optical coherence tomography imaging [J]. Journal of Biomedical Optics, 2013, 18(2): 026004.
- [26] Lee C Y, Wang H J, Jhang J D, et al. Automated *drosophila* heartbeat counting based on image segmentation technique on optical coherence tomography[J]. Scientific Reports, 2019, 9: 5557.
- [27] Sawyer T W, Rice P F S, Sawyer D M, et al. Evaluation of segmentation algorithms for optical coherence tomography images of ovarian tissue[J]. Journal of Medical Imaging, 2019, 6(1): 014002.
- [28] Cao Y H, Cheng K, Qin X J, et al. Automatic lumen segmentation in intravascular optical coherence tomography images using level set [J]. Computational and Mathematical Methods in Medicine, 2017, 2017: 4710305.
- [29] Saratxaga C L, Bote J, Ortega-Morán J F, et al. Characterization of optical coherence tomography images for colon lesion differentiation under deep learning [J]. Applied Sciences, 2021, 11(7): 3119.
- [30] Meiburger K M, Salvi M, Rotunno G, et al. Automatic segmentation and classification methods using optical coherence tomography angiography (OCTA): a review and handbook[J]. Applied Sciences, 2021, 11(20): 9734.
- [31] Guo M L, Zhao M, Cheong A M Y, et al. Automatic quantification of superficial foveal avascular zone in optical coherence tomography angiography implemented with deep learning[J]. Visual Computing for Industry, Biomedicine, and Art, 2019, 2(1): 21.
- [32] Liu J, Yan S X, Lu N, et al. Automatic segmentation of foveal avascular zone based on adaptive watershed algorithm in retinal optical coherence tomography angiography images[J]. Journal of Innovative Optical Health Sciences, 2022, 15(1): 1-13.
- [33] Zhao H S, He B, Ding Z Y, et al. Automatic lumen segmentation in intravascular optical coherence tomography using morphological features[J]. IEEE Access, 2019, 7: 88859-88869.
- [34] Rahman M H, Jeong H W, Kim N R, et al. Automatic quantification of anterior lamina cribrosa structures in optical

- coherence tomography using a two-stage CNN framework [J]. Sensors, 2021, 21(16): 5383.
- [35] Valerio T. Automated algorithm for optical coherence tomography (OCT) images of 3D spheroids [D]. Oklahoma: University of Oklahoma, 2020: 1-18.
- [36] 买童童, 魏丽亚, 姚晓天, 等. 基于光学相干层析技术的昆虫胚胎影像处理方法 [J]. 中国激光, 2021, 48(9): 0907002.
- Mai T T, Wei L Y, Yao X T, et al. Image processing method of an insect embryo based on optical coherence tomography [J]. Chinese Journal of Lasers, 2021, 48(9): 0907002.
- [37] Wang Z, Benjamin P, Chen L, et al. Cubic meter volume optical coherence tomography [J]. Optica, 2016, 3(12): 1496-1503.

Automatic Detection and Quantitative Analysis of Insect Cardiac Function Parameters Using OCT

Wang Xiuli^{1,2}, Du Ruoxuan¹, X. Steve Yao^{1,2}, Su Ya^{1,2,3*}, Cui Shengwei^{1,2,3}, Hao Peng^{1,2}, Yang Lijun¹, Duan Bingbing^{1,2}

¹ College of Physics Science & Technology, Hebei University, Baoding 071002, Hebei, China;

² Hebei Provincial Center for Optical Sensing Innovations, Baoding 071002, Hebei, China;

³ Institute of Life Science and Green Development, Hebei University, Baoding 071002, Hebei, China

Abstract

Objective Cardiovascular is one of the major diseases that threatens human health, and the prevalence of cardiovascular disease in China continues to grow. Therefore, it is important to select an appropriate model organism to understand the development of the heart. Locust has the characteristics of easy operation, strong plasticity, and short development cycle as well as the similar gene regulation mechanism with human beings in the process of cardiac development, therefore it becomes a useful candidate for studying the cardiac function and for the pathological gene analysis. Researchers have proposed a variety of methods to evaluate the heart function of insects, such as multi-sensor electrocardiogram, atomic force microscope monitoring, and electrical stress method. However, these methods are invasive and cannot monitor the same living body continuously. Therefore, a method which can monitor the heart development and screen the phenotypic variation of insects or other model organisms non-invasively is more desired. Fortunately, optical coherence tomography (OCT), widely used in biomedical detection because of its noninvasiveness, real-time, and high resolution, can be used to detect the internal structures of biological tissues and other non-uniform scatterers. Therefore, it is a more suitable tool to monitor the embryonic heart development of a locust. In addition, the measurement of cardiac function parameters (such as heart rate) still needs to be calculated manually by the M-Mode diagram, which is not only time-consuming but also prone to errors. Therefore, a high efficiency automatic detection algorithm is a critical issue to be solved urgently in the high-throughput screening and phenotypic analysis of model biological pathogenic genes.

Methods Using a locust as the model organism, in our previous works we have monitored the embryo development and screened the phenotypic variation caused by the RNAi technology. Here, a new method is proposed to automatically and quickly calculate the insect heart function parameters, such as end diastolic diameter (EDD), end systolic diameter (ESD), end diastolic area (EDA), end systolic area (ESA) and heart rate (HR). The processing flow is shown in Fig. 2. The collected 3D data are expanded in time series to obtain the M-Mode diagram of the embryo heart chamber. After gray-scale transformation of the M-Mode diagram, by a series of operations including threshold-segmentation-based regional growth, boundary recognition, morphological processing, and feature peak extraction, the parameters including HR, EDD and ESD can be obtained.

Results and Discussions The low-frequency noise in the original M-Mode image [Fig. 3(a)] is removed after gray-scale transformation [Fig. 3(b)], which is beneficial for the calculation by the regional growth algorithm. Then, any point selected in the fetal heart ventricle [the red dot in Fig. 3(c)] can be used as the initial seed point, and the binary regional growth result can be obtained under the specified regional growth criterion [Fig. 3(d)]. As shown in Fig. 3(d), there are burrs at the edge of the ventricle caused by the non-uniformity of the grayscale distribution, which adversely influences the accuracy in obtaining the heart beat amplitude in the next step. To solve this problem, morphological processing is introduced, which plays a good role in smoothing the cavity edge. The image after removing burrs is shown in Fig. 3(e). By counting the numbers of pixels with the logical value of 0 in A-scan and knowing the size of single pixel, the beat amplitude of the heart at different moments can be obtained [Fig. 3(f)]. As shown in Fig. 3(g), the HR, EDD, and ESD cardiac parameters can be calculated after the extreme points are found by the peak extraction algorithm. If the original image is changed from the M-Mode image to the B-scan image of the cross section of the embryonic heart, the

maximum EDA and the minimum ESA of the locust embryonic heart can be calculated according to the steps in section 2.2, as shown in Fig. 6. Therefore, one can automatically detect and quantitatively analyze the heart function parameters of insect embryos by the proposed algorithm.

Conclusions In the field of heart development and mechanism of heart disease, OCT has been successfully applied to detect the heart function of model organisms such as insects due to its advantages of noninvasiveness, real-time, and high resolution. However, the detection algorithm still has some problems, such as low efficiency, high requirements on image quality, and inaccuracy of measurement, especially it is not suitable for the detection under a large sample size. In this paper, we propose a high speed automatic detection and quantitative analysis algorithm of insect cardiac function parameters by OCT. The position of the seed point is determined through human-computer interaction, and a series of processing such as automatic image segmentation and target region division are performed on the OCT M-Mode image of the insect heart. The proposed algorithm can quickly and accurately measure the cardiac function parameters including the end diastolic diameter, end systolic diameter, end diastolic area, end systolic area, and heart rate. This method can improve the screening and analysis efficiency of pathogenic genes in high-throughput biological samples and has important applicable value in the research of cardiovascular disease using insects as model organisms.

Key words biotechnology; optical coherence tomography; insect; model organism; cardiac function parameters